Food Chemistry: X 23 (2024) 101696

Contents lists available at ScienceDirect

Food Chemistry: X

journal homepage: www.sciencedirect.com/journal/food-chemistry-x

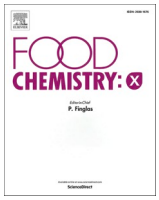

Uncovering quality changes of shrimp (*Penaeus vannamei*) during solar drying and its relationship with protein-related properties

Xinyue Pan [1], Jiarong Wang [1], Wenya Xu, Jie Wang, Jianfeng Sun, Wenxiu Wang [*], Yiwei Tang [*]

College of Food Science and Technology, Hebei Agricultural University, Baoding 071000, China

ARTICLE INFO

Keywords:
Solar drying
Penaeus vannamei
Protein oxidation
Protein denaturation
Protein degradation
Quality attribute
Correlation analysis

ABSTRACT

This study explored the intrinsic relationship between the quality traits and protein-related property changes during the solar drying of shrimps (*Penaeus vannamei*). During drying, the shrimp exhibited a gradual decline in $L^*a^*b^*$ values and a notable increase in the hardness and chewiness. Proteins were degraded and oxidized. Especially, the trichloroacetic acid-soluble peptide and carbonyl contents increased, whereas the total sulfhydryl content decreased. The proportions of different types of intramolecular bonds were significantly changed. The ionic and hydrogen bonds greatly decreased to 10.72% and 9.05% and the hydrophobic and disulfide bonds notably increased to 19.38% and 28.19%, indicating the changes in the spatial structure of the protein and its denaturation during the drying process. The Pearson's correlation analysis showed that protein degradation and denaturation greatly affected the textural properties and protein oxidation caused color changes. The result of this work provides a theoretical support for improving the quality of shrimp products.

1. Introduction

Penaeus vannamei, one of the three most productive farmed shrimp species in the world, has become a major farmed species in China (Wang, Che, & Sun, 2022). Shrimps are highly susceptible to spoiling and have short shelf life owing to their high moisture content, sensitive texture, low connective tissue proportion, and high-level enzyme activity at ambient temperatures (Wang, Zhang, & Mujumdar, 2011). Therefore, drying is among the most important shrimp processing methods for shelf life extension while ensuring unique flavor, high nutritional value, and ambient-temperature storage (Li et al., 2020). Widely used traditional drying methods, such as sun and hot-air drying, are time- and energy-consuming. Although emerging technologies, such as vacuum-freezing, microwave treatment, and combination drying, can yield high-quality products, the required investment in the equipment and high energy consumption limit their industrial applications (Li, Zhu, Sun, Sang, & Yang, 2016). Therefore, solar drying is attracting widespread attention owing to its low energy requirements and environmental sustainability. Combined with heat-pump drying, solar drying addresses the problem of insufficient energy supply and allows for improved temperature and humidity control for enhanced efficiency and dried product quality (Wang et al., 2022; Wang, Che, & Sun, 2022).

Protein properties, related to the primary component of shrimp muscles, are closely correlated to dried shrimp product quality. Previous studies confirmed that common processing methods, such as steaming, boiling, drying, and frying, could alter the shrimp protein content. Moreover, boiling duration and salt solution concentration could affect shrimp texture. Gao et al. (2016) discovered that the protein content in *Penaeus vannamei* shrimp started to change after heating at 50 °C for 10 min, resulting in reduced α-helix and increased β-fold ratios. Consequently, the physical properties of the muscle tissue changed with the alterations in the hydrogen and hydrophobic bonds during heating. Zhang et al. (2023) compared how drying, steaming, and microwaving affect shrimp properties, noting that the carbonyl group of the myofibrillar proteins increased and the sulfhydryl content decreased upon heat treatment, indicating protein oxidation. Duppeti, Manjabhatta, and Kempaiah (2023) further reported the effect of protein denaturation and heat treatment-related structural aggregation on the functional

Abbreviations: L^*, lightness component; a^*, green–red-light color component; b^*, blue-light color component; ΔE, total color difference; SDS-PAGE, sodium dodecyl sulfate-polyacrylamide gel electrophoresis; TCA, trichloroacetic acid.

* Corresponding authors.
E-mail address: cauwwx@hebau.edu.cn (W. Wang).

[1] These authors contributed equally to this work and should be considered co-first authors

https://doi.org/10.1016/j.fochx.2024.101696
Received 20 March 2024; Received in revised form 19 July 2024; Accepted 22 July 2024
Available online 25 July 2024
2590-1575/© 2024 Published by Elsevier Ltd. This is an open access article under the CC BY-NC-ND license (http://creativecommons.org/licenses/by-nc-nd/4.0/).

properties of proteins as well as food texture and flavor.

Solar drying consists of two phases: blanching pretreatment and drying. During blanching, proteins undergo thermal denaturation with increasing processing temperatures, resulting in changes in important properties, such as solubility, elasticity, and chewiness, thereby affecting product texture and flavor (Haritha, Nakkarike Manjabhatta, & Bheemanakere Kempaiah, 2023). During drying, protein property changes intensify as moisture is continuously eliminated from the shrimp, influencing product characteristics, such as color and texture (Akonor, Ofori, Dziedzoave, & Kortei, 2016). During solar drying, protein denaturation, oxidation, and degradation are closely related to shrimp quality. However, the dominant factor for such changes under the synergistic heat treatment and dehydration effects remains unclear. Therefore, an in-depth analysis would be required to investigate the correlation between protein changes and product properties during shrimp drying and provide a theoretical basis for product quality improvement.

Therefore, in this study, we aimed to explore how protein changes potentially affect the physiochemical properties changes of *Penaeus vannamei* during solar drying. We used Pearson's correlation analysis to unravel the intrinsic relationship between protein changes and product properties, offering key information for advancing the theory of regulating solar-dried shrimp product quality.

2. Materials and methods

2.1. Materials

Sodium hydroxide, acetic acid, ethyl acetate, and other chemical reagents, which are all of analytical grade, were purchased from Tianjin Tianli Chemical Reagent Co., Ltd. (China).

2.2. Sample preparation

The optimal experimental conditions for the solar drying of shrimps (*Penaeus vannamei*) were based on our previous study (Guo et al., 2017) with slight modifications. Live shrimps (*Penaeus vannamei*), weighing approximately 11.62 ± 2.2 g, were purchased in October 2021 from the Science and Technology Market of Hebei Agricultural University in Baoding City. The foreign substances on the shrimp surface were cleaned. Subsequently, the shrimps were boiled in water with 3 mass% salt for 70 s according to our previous study (Xu et al., 2023). The ratio of the material to water is 1:1.5. The scalded shrimps were drained, laid in a plastic tray, and placed in a solar drying equipment (Zhangjiakou Taihua Machinery Factory, Hebei province, China). The solar drying process parameters were set to a temperature of 55 °C, wind speed of 8 m/s, and load capacity of 3 kg. Fresh, scalded, and dried shrimps were selected as experimental samples. The shrimps were dried with a treatment time of 12 h, and samples were obtained every 2 h to determine the physicochemical indexes and protein change indicators.

2.3. Determination of moisture, crude protein, and crude fat content

Moisture was determined according to the direct drying method described in the National Standard of China (GB 5009.3–2016). The weighing dishes were weighted as approximately 2.00 g by a CP214 analytical balance (Qin, Wang, Wang, & Shi, 2020) before the experiment. Subsequently, the total mass of the bottles and shrimp samples were weighted. The samples were placed in an oven at 105 °C to achieve constant weight and a dryer to cool for 30 min. Finally, the quality before and after drying was obtained. Crude protein was determined according to the Kjeldahl nitrogen method in the National Standard of China (GB 5009.5–2016). Crude fat was obtained according to the Soxhlet extraction method of the National Standard of China (GB 5009.6–2016).

2.4. Determination of the dry-basis moisture content and drying rate

The dry-basis moisture content (W_R) was calculated as:

$$W_R(\%) = \frac{m_1}{m_2} \times 100 \quad (1)$$

where m_1 is the moisture of shrimp (g), and m_2 is the mass of the dry material (g) of the shrimp at a certain drying time.

The drying rate (D_R) was calculated as

$$D_R(\%) = \frac{W_{t1} - W_{t2}}{t_1 - t_2} \times 100 \quad (2)$$

where t_1 and t_2 are different drying times (h); and W_{t1} and W_{t2} are the dry water content of the shrimps at t_1 and t_2, respectively (%).

2.5. Low field magnetic resonance (LF-NMR) measurements

To monitor the dynamic water state and migration, relaxation time (T_2) and magnetic resonance imaging (MRI) were analyzed using an NMI20 LF-NMR analyzer (NMI20-060H-I-40 mm, NIUMAG Electronic Technology Co., Ltd., Shanghai, China). Whole shrimp samples were placed in cylindrical glass tubes, and the Carr-Purcell-Meiboom-Gill (CPMG) decay signals were collected using a radio-frequency (RF) coil with a diameter of 40 mm. The transverse relaxation time of the samples was measured, and T_2 inversion software was used to obtain the T_2 inversion spectrum. The parameter settings were as follows: main frequency, 21 MHz; RF delay, 0.02 ms; 90- and 180-degree pulse widths, 10.60 μs and 18.24 μs, respectively; sampling frequency, 250 kHz; cumulative number of times, 2. Each sample was measured three times to obtain the average value, ultimately resulting in the relaxation time and peak area of the shrimp samples with different drying times, as well as those of the boiled and fresh shrimp.

For MRI analysis, after calibrating with standard samples, the shrimp samples were placed in the magnet cavity, and water distribution imaging was acquired using MRI software. The parameter settings were as follows: field of view (FOV) = 100 mm × 100 mm, slice width = 1.1 mm, slice gap = 1.1 mm; average = 2; read size = 256; phase size = 192; T_2-weighted image echo time (TE) = 20 ms; repetition time (TR) = 500 ms.

2.6. Color determination

The second and third ventral segments of the shrimp were used for the color measurement. Luminance (L^*), green–red color component (a^*; +a, redness; −a, greenness), and blue–yellow color component (b^*; +b, yellowness; −b, blueness) were measured by a CR-400 colorimeter. All experiments were conducted five times. The color difference value ΔE was obtained by the following formula (Li, Zhou, Yin, Dong, & Shahidi, 2020).

$$\Delta E = \sqrt{\left(L^* - L_0^*\right)^2 + \left(a^* - a_0^*\right)^2 + \left(b^* - b_0^*\right)^2} \quad (3)$$

The color evaluation was conducted according to the National Bureau of Standards, whereby the absolute value of 1 as a unit is called the "NBS color difference unit". The relationship between the NBS unit chromatic aberration values and observed sensations can be categorized based on the ΔE value. If $\Delta E < 0.5$, the sensation is considered as "trave". If $0.5 < \Delta E < 1.5$, the sensation is classified as "slight". If $1.5 < \Delta E < 3.0$, the sensation is categorized as "noticeable". If $3.0 < \Delta E < 6.0$, the sensation is considered as "appreciable". Finally, if $\Delta E > 6$, the sensation is described as "excessive".

2.7. Texture determination

The shrimps with the shell removed were subjected to texture analysis. The hardness, elasticity, and chewiness were detected by a Texture

Expert software (TMS-Pro, Food Technology Corp., Sterling, VA, USA) using a cylindrical probe with a diameter of 75 mm, measurement speed of 30 mm/s, deformation variable of 60%, and an interval of 0 s between compressions (Xu et al., 2022).

2.8. Microstructure determination

The first two sections of the shrimp were cut into cubes with a side of 4 mm. The cubes were immersed in 2.5% glutaraldehyde buffer and fixed at 4 °C for 24 h. Subsequently, they were washed with phosphate buffer solution (0.1 mol/L, pH 7.2) thrice for 15 min each and eluted with 10%, 20%, 40%, 60%, and 80% ethanol solution for 20 min. The samples were pre-frozen at −80 °C for 10 h and then lyophilized. The dried samples were sprayed with gold and observed under scanning electron microscopy (Fei Tecnai F20, USA) with the following parameters: vacuum of 10 Pa, discharge current of 20 mA, gold spray time of 150 s, and magnification of 1000 (Zhu, Zhang, Zhao, Wu, & Qiao, 2020).

2.9. Trichloroacetic acid (TCA)-soluble peptide content determination

The TCA-soluble peptide content was determined using a method modified from a previous work (Li et al., 2020). Precooled 5% (*w/v*) TCA solution (27 mL) was added to the sample (3.0 g). The mixture was homogenized and kept at 4 °C for 1 h. Subsequently, it was centrifuged at 10,000*g* at 4 °C for 15 min. The supernatant was obtained to determine the soluble peptides using a Folin-phenol reagent (Tianjin Guangfu Technology Development Co., Ltd. China).

2.10. Sodium dodecyl sulfate-polyacrylamide gel electrophoresis (SDS-PAGE) analysis

The sample was accurately weighted to 0.1 *g* in a centrifuge tube containing 1 mL PIPA lysate, homogenized in an ice bath in a high-throughput tissue grinder (Ningbo Xinzhi Biotechnology Co., Ltd. Zhejiang province, China), and incubated with ice water for 20 min (Xu et al., 2023). The mixture was then centrifuged at 14,000*g* for 10 min to obtain a stock solution with myofibrillar protein as the supernatant. The protein concentration was determined using the BCA Protein Quantitation Kit, and all protein samples stock were diluted to the same suitable concentration by a PIPA lysate. The obtained myofibrillar protein solution was mixed with loading buffer according to the volume ratio of 4:1 and heated in boiling water for 5 min. The mixture was added to the SDS-PAGE gels, subjected to electrophoresis at 130 V with a constant pressure for approximately 100 min, stained with staining buffer for 30 min, and decolorized with distilled water. Finally, the molecular quality of the protein was determined by comparison with a protein marker (10–250 kDa).

2.11. Protein carbonyl determination

Carbonyl content was measured as described by (Koutina, Jongberg, & Skibsted, 2012). The protein carbonyl content in shrimp meat was determined using the dinitrophenylhydrazine (DNPH) colorimetric method. The sample was accurately weighed to 2.00 g and placed in 10 mL of 0.02 mol/L phosphate buffer (pH 6.5, containing 0.6 mol/L NaCl). The mixture was centrifuged at 13000*g* for 10 min, and 400 μL supernatant was transferred into an Eppendorf tube. Subsequently, 200 μL of 2 mol/L HCl (containing 0.01 mol/L DNPH) was added to the mixture, vortexed and mixed, placed in a dark water bath at 30 °C for 1 h, added with 1 mL of 40% TCA, mixed, and kept for 30 min to precipitate the protein. The mixture was centrifuged at 130000 r/min for 15 min, and the supernatant was discarded. In the pellet, 1 mL mixture of ethyl acetate and ethanol was dissolved (mixing ratio of 1:1) to remove excess DNPH. This step was repeated until the supernatant is colorless. Finally, solids were dissolved in 3 mL of 6 mol/L guanidine hydrochloride solution, and the absorbance of the solution was measured at a wavelength of 370 nm. The protein concentration was determined using the BCA kit (Beijing Solarbio Science & Technology Co., Ltd. China). The trial was repeated thrice. The protein carbonyl content (nmol/mg) was calculated according to the equation:

$$X(\text{nmol/mg}) = \frac{A_{370\text{nm}}}{a \times b \times c} \times 10^6 \quad (4)$$

where $A_{370\text{nm}}$ is the absorbance of the measured solution, a is the absorbance coefficient of carbonyl molecules (22,000 L/(g·cm)), b is the optical path (1 cm), and c is the protein concentration (mg/mL).

2.12. Total sulfhydryl determination

The total sulfhydryl content was determined by dissolving 0.5 g sample in 3 mL of extract and followed by centrifugation on ice at 8000*g* and at 25 °C for 10 min. The total sulfhydryl content in the supernatant was determined using a detection kit (Beijing Solarbio Science & Technology Co., Ltd. China) (Li, Zhou, Zhang, Su, & Shui, 2021).

2.13. Determination of the intermolecular interaction forces

The intermolecular interaction forces of protein were measured according to (Tong et al., 2023) with slight modifications. Approximately 2.0 g sample was placed in 10 mL of 0.6 mol/L NaCl (S1) and centrifuged at 5000*g* for 2 min. The mixture was stored at 4 °C for 1 h and then centrifuged at 4 °C and 8500*g* for 30 min. Subsequently, the supernatant was taken. A mixture of 1.5 mol/L urea and 0.6 mol/L NaCl (10 mL) was added to the centrifuge pellet, forming a mixture (S2) treated in the same manner as previously described. Subsequently, a mixture of 8 mol/L urea and 0.6 mol/L NaCl (10 mL) was added to the centrifuged pellet to form another mixture (S3), which was subjected to the same treatment. Finally, a mixture of 0.5 mol/L β-mercaptoethanol, 8 mol/L urea, and 0.6 mol/L NaCl (10 mL) was added to the above centrifuged pellet (S4), which was also treated in the same manner. The protein concentration in the supernatant was determined using the BCA protein quantitation kit method. After extracting the S1, S2, S3, and S4 extracts, the protein concentrations of the supernatant correspond to the contents of ionic bonds, hydrogen bonds, hydrophobic bonds, and disulfide bonds, respectively.

2.14. Statistical analysis

The experimental results were expressed as mean ± standard error. One-way analysis of variance method and multiple comparison (Duncan method) with SPSS (version 27.0; SPSS Inc., Chicago, IL, USA) was used to establish the regression model using the multiple linear regression method. The plots were produced using Origin2021 (The OriginLab Inc., Northampton, MA, USA).

3. Results and discussion

3.1. Physiochemical changes in the shrimp during drying

3.1.1. Moisture, protein, and fat contents

Table 1 presents the moisture, protein, and fat contents of shrimp during solar drying. After 10 h of drying, the moisture content decreased from 75.65% to 15.67%, reaching the national standard of <25% (SC/T3220–2016). Low water activity effectively inhibits microorganism growth and prolongs shelf life (Beuchat et al., 2013). The protein content increased from 20.13 g/100 g to 73.56 g/100 g, which is significantly higher than that of the fresh and blanched samples ($p < 0.05$), owing to the crude protein enrichment during dehydration. Finally, the fat content increased from 0.98 g/100 g to 2.50 g/100 g.

Table 1
Moisture content, protein, fat, color changes and comparison of the color difference values based on the dry shrimp samples.

Drying time (h)	Moisture content (g/100 g)	Protein (g/100 g)	Fat (g/100 g)	L*	a*	b*	ΔE												
							Fresh	Boiled	1	2	3	4	5	6	7	8	9	10	11
Fresh	75.65 ± 0.13^{a}	20.13 ± 0.71^{n}	0.98 ± 0.01^{i}	40.88 ± 2.57^{g}	1.30 ± 0.34^{f}	5.50 ± 1.30^{g}	–												
Boiled	72.75 ± 0.06^{b}	22.58 ± 0.25^{m}	1.14 ± 0.01^{h}	64.26 ± 1.23^{ab}	22.54 ± 1.53^{a}	27.99 ± 1.97^{a}	38.83	–											
1	69.46 ± 0.12^{c}	28.67 ± 0.336^{l}	1.19 ± 0.02^{gh}	65.37 ± 0.96^{a}	19.4 ± 0.95^{b}	25.06 ± 1.72^{b}	36.23	4.76	–										
2	63.81 ± 0.16^{d}	32.38 ± 0.62^{k}	1.24 ± 0.01^{gh}	63.73 ± 0.70^{ab}	19.41 ± 1.00^{b}	24.43 ± 1.53^{bc}	34.79	4.94	2.58	–									
3	56.76 ± 1.26^{e}	35.86 ± 0.319^{j}	1.27 ± 0.01^{gh}	64.13 ± 1.48^{ab}	16.84 ± 1.52^{cde}	22.21 ± 1.60^{de}	32.65	8.39	4.57	4.04	–								
4	51.56 ± 1.27^{f}	40.54 ± 0.41^{i}	1.29 ± 0.01^{gh}	62.91 ± 2.03^{bc}	18.02 ± 1.08^{bc}	22.59 ± 1.87^{cd}	32.61	7.58	4.56	3.64	3.26	–							
5	45.24 ± 1.1^{g}	46.92 ± 0.232^{h}	1.44 ± 0.03^{f}	61.38 ± 2.34^{cd}	16.87 ± 1.67^{cde}	21.47 ± 2.17^{def}	30.46	9.62	6.79	5.63	4.26	4.01	–						
6	41.92 ± 0.72^{h}	52.33 ± 0.52^{g}	1.67 ± 0.01^{e}	60.47 ± 1.87^{de}	16.76 ± 1.86^{cde}	19.94 ± 1.66^{f}	28.96	10.94	8.00	6.68	5.00	4.62	3.27	–					
7	39.27 ± 0.96^{i}	55.86 ± 0.534^{f}	1.76 ± 0.09^{e}	58.29 ± 0.91^{f}	15.71 ± 1.22^{de}	20.74 ± 1.05^{def}	27.31	11.72	9.23	7.72	6.34	5.73	3.76	2.95	–				
8	33.17 ± 0.55^{j}	61.54 ± 0.22^{e}	1.99 ± 0.10^{d}	57.81 ± 2.56^{f}	16.19 ± 1.28^{de}	22.12 ± 2.63^{de}	28.19	11.33	9.38	7.97	7.13	6.50	5.14	4.97	3.95	–			
9	29.14 ± 0.86^{k}	64.34 ± 0.477^{d}	2.14 ± 0.04^{c}	59.44 ± 1.63^{def}	15.91 ± 1.06^{de}	19.79 ± 1.74^{f}	27.67	11.77	8.87	7.47	5.66	5.28	3.39	2.74	2.94	3.71	–		
10	23.49 ± 0.04^{l}	68.54 ± 0.41^{c}	2.33 ± 0.11^{b}	58.64 ± 1.94^{ef}	15.89 ± 0.92^{de}	20.37 ± 1.15^{ef}	27.46	11.79	9.14	7.68	6.10	5.60	3.61	2.82	2.30	2.99	2.30	–	
11	20.51 ± 0.75^{m}	71.07 ± 0.155^{b}	2.44 ± 0.07^{a}	58.52 ± 1.55^{ef}	15.31 ± 1.41^{e}	21.18 ± 1.36^{def}	27.52	11.63	9.09	7.64	6.25	5.73	3.95	3.61	2.45	2.62	2.99	2.61	–
12	15.67 ± 0.12^{n}	73.56 ± 0.22^{a}	2.50 ± 0.15^{a}	58.06 ± 1.97^{f}	17.06 ± 1.29^{cd}	20.69 ± 1.89^{def}	27.90	11.23	9.08	7.48	6.71	5.81	4.32	3.73	3.11	3.31	3.33	3.07	3.39

Note: Mean values with different letters within each column are significantly different ($p < 0.05$).

3.1.2. Dry-basis moisture contents and drying rate

Fig. 1 summarizes the changes in the dry-basis moisture content and drying rate during shrimp drying. After 2 h of drying, the relative dry-basis moisture content decreased from 300.43% to 167.63%, representing an increased drying rate and implying a fast drying process during the initial phase. The shrimp surface moisture dramatically evaporated with an increase in shrimp surface temperature. After drying for 2–6 h, the dry-basis moisture content decreased to 64.47%, coupled with a gradual reduction in the drying rate. This may be because, at this stage, the free water had completely evaporated, causing the surface temperature of the shrimp to stabilize. Immobilized water begins to diffuse outward, dominating the drying process. The internal moisture rapidly migrated toward the exterior with a decreasing interior pressure gradient in the shrimp samples. However, the hindered interior moisture evaporation caused by the hardening of the shrimp surface progressively decreased the drying rate. Similar moisture trends were observed by Shaheed, Jafor, Nazrul, and Kamal (2009), who described rapid initial drying of seafood fillets at 50–55 °C due to surface moisture evaporation, followed by a decrease in drying rate as internal moisture movement to the surface slowed down until reaching stability. During the final phase, the drying rate remained relatively constant, and the final dry basis moisture content was 24.56%, indicating that protein denaturation during the drying process led to structural alterations in the muscle tissue and reduced water retention (Shi et al., 2017). The exterior and interior moisture gradients of the shrimp samples reached equilibrium, reducing the interior moisture diffusion, evaporation, and drying rates.

3.1.3. LF-NMR analysis

The moisture distribution inversion curves of the shrimp samples with different drying times were obtained using LF-NMR (Fig. 1B), and the T_2 was closely related to the food moisture distribution state and kinetics. The smaller the T_2 value of the sample, the smaller the distance between the protons, indicating tighter water-matrix binding. To better characterize the water state in the shrimp samples, the relaxation times T_{20}, T_{21}, T_{22}, and T_{23} were defined as strongly bound water tightly associated with macromolecules at approximately 0.01–2 ms, weakly bound water associated with or trapped in highly organized structures at approximately 2–10 ms, immobilized water tightly bound to muscle fibers at approximately 10–100 ms, and free water at approximately 100–10,000 ms, respectively. The strongest T_2 signal amplitude was emitted by raw shrimp, followed by boiled shrimp. As drying time increased, the transverse relaxation time of T_{20} exhibited minimal shift to the left, from 1.10 ± 0.09 ms to 0.20 ± 0.05 ms, indicating that the duration of drying has minimal effect on strongly bound water, whose degree remained almost unchanged. In contrast, the transverse relaxation time of T_{22} decreased significantly, and the degree of freedom of immobilized water gradually decreased, likely owing to the gradual contraction of the muscle fiber structure caused by heating. After six hours of drying, the signal strength of T_{23} was 0 ms, indicating complete evaporation of free water.

As the signal amplitude peak area of the T_2 relaxation time for hydrogen protons is proportional to the water content, it can be used to estimate the water content of the sample. As shown in Supplementary Table S1, the peak areas of amplitude signals were normalized to obtain the peak areas of strongly bound water (A_{20}/g), weakly bound water (A_{21}/g), immobilized water (A_{22}/g), free water (A_{23}/g), and total peak area (A_{Total}/g) per unit of mass at different drying times of shrimp. With extended drying time, the total peak area decreased continuously. Specifically, the peak areas of A_{23} and A_{22} decreased to 0 after 6 h and 12 h, respectively, indicating that the drying process mainly involved the loss of free water and less mobile water. The value of A_{21} initially decreased, then increased, and subsequently decreased. This pattern, combined with the relaxation time of T_{22}, indicates that the relaxation curve shifted to the left, suggesting an overlap between T_{21} and T_{22}. This may be due to the fact that at this point the fascicles became thinner and fractured, and the fiber network structure is disrupted, thus blurring the boundary between bound and fixed water and making the distinction between T_{21} and T_{22} less obvious. During the drying process, most of the immobilized water evaporated continuously, with a small portion converted into bound water, leading to a consistent increase in the peak area of strongly bound water. Consistent with our results, Li, Guan, Ge,

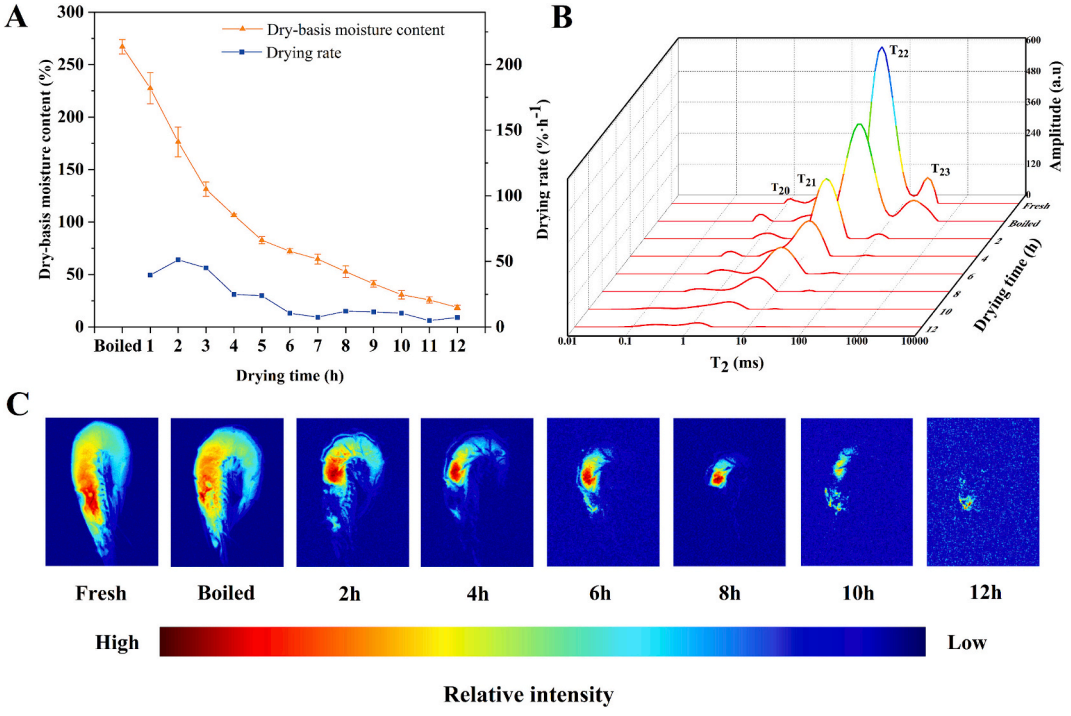

Fig. 1. Changes in (A) the dry-basis moisture content and drying rate, (B) spin relaxation time (T_2), and (C) T_2-weighted MRI images of *Penaeus vannamei* during the drying process.

Zhang, and Ling (2020) investigated heat pump drying of tilapia fillets and reported that water-solid binding strength increased with the progressing drying process and high-to-low degree of freedom water migration.

Fig. 1C presents the MRI imaging of shrimps during the drying process, where the red color represents high-intensity hydrogen proton signals, while the blue color represents low-intensity hydrogen proton signals. The brighter areas gradually decreased with increasing drying times, the red areas gradually changed to blue, and the blue areas gradually decreased from the outside to the inside, indicating a significant signal intensity and water content reduction. Consistent with our results (Fig. 1A, B), Xu et al. (2023) observed a similar phenomenon in the regional color change when investigating the shrimp hot air drying process using MRI imaging. These results underscore that mainly free water and water with reduced mobility are lost during the drying process.

3.1.4. Color changes during shrimp drying

Table 1 summarizes the color changes during shrimp drying. Fresh shrimp color changed to orange after blanching, gaining a golden hue during drying. The L^*, a^*, and b^* values increased during blanching, and all three values decreased upon drying from 64.26, 22.54, and 27.99 to 58.06, 17.06, and 20.69, respectively. The significant increase in the L^* value during blanching was related to temperature-induced complete myosin and actin denaturation, similar to the results reported by Niamnuy, Devahastin, and Soponronnarit (2007), who established that protein degradation during blanching contributes to astaxanthin release of from the carotenoid-protein complex, thereby increasing both the a^* and b^* values. In contrast, the reduction in the L^* value during drying occurred owing to the Maillard reaction between the carbonyl and free amino groups (Guo et al., 2022).

Table 1 also provides a comparison of the color differences between several dried samples. The total color difference (ΔE) calculation, using fresh shrimp as a reference, revealed a decreasing trend during the drying process. However, the ΔE values always remained higher than 27, indicating that the dried shrimp color significantly differed from that of fresh shrimp. Subsequently, the ΔE values of the dried shrimp at later time points were calculated using the shrimp samples at each stage as a reference. The results revealed that the ΔE value increased during drying and was higher than 2, indicating considerable color changes between the initial and drying stages. The ΔE values were all below 6 between 6 and 12 h of drying, suggesting the gradually weakened but noticeable color changes.

3.1.5. Textural changes

Table 2 presents the textural changes in the shrimp samples during drying. The hardness increased from 106.38 to 394.30 N,. This result is potentially attributed to the gradual water loss, actin and myosin dissociation, muscle fiber disintegration, and myofibril dissociation and small fragment formation, thereby increasing muscle fiber structure hardness, destroying the protein structure, and eventually causing surface sclerosis (Emilia Latorre & Ezequiel Velazquez, 2021). After blanching, the elasticity increased from 0.83 to 1.83 mm and continued to rise, reaching a peak of 2.38 mm after 8 h of drying. Owing to the continuous evaporation of immobilized and weakly bound water, muscle tissue rapidly contracts, causing irreversible deformation, denaturation, and aggregation of proteins, ultimately resulting in a constant loss of elasticity. Stickiness initially increased, then decreased, reaching a maximum of 45.59 mJ at 8 h. In contrast, chewiness increased gradually. Stickiness and chewiness are comprehensive textural characteristics affected by various parameters. In our study, the increase in shrimp product hardness enhanced stickiness and chewiness. Dong et al. (2020) reached the same conclusion, reporting increased prawn hardness and chewiness with prolonged cold-air drying time and appropriately increased chewiness associated with improved taste.

Table 2
Changes in the texture of *Penaeus vannamei* during the drying process.

Drying time (h)	Hardness (N)	Elasticity (mm)	Adhesiveness (mJ)	Chewiness (mJ)
Fresh	106.38 ± 4.13^{l}	0.83 ± 0.03^{e}	2.75 ± 0.10^{j}	3.03 ± 0.08^{h}
Boiled	116.14 ± 10.31^{l}	1.83 ± 0.04^{d}	12.83 ± 0.28^{i}	23.3 ± 0.88^{g}
1	143.49 ± 2.07^{k}	1.79 ± 0.04^{d}	16.64 ± 0.47^{hi}	30.7 ± 1.87^{fg}
2	174.22 ± 9.72^{j}	1.81 ± 0.07^{d}	19.53 ± 1.69^{gh}	32.55 ± 3.37^{fg}
3	189.92 ± 11.87^{i}	1.80 ± 0.05^{d}	21.89 ± 1.59^{fg}	37.94 ± 1.23^{f}
4	206.18 ± 18.00^{h}	1.89 ± 0.06^{cd}	19.10 ± 0.54^{gh}	48.85 ± 2.85^{e}
5	219.36 ± 16.31^{h}	2.02 ± 0.03^{bc}	24.24 ± 1.86^{f}	57.29 ± 2.27^{e}
6	236.34 ± 13.65^{g}	2.02 ± 0.04^{bc}	34.88 ± 3.63^{e}	79.15 ± 3.22^{d}
7	261.17 ± 15.90^{f}	2.08 ± 0.08^{b}	36.77 ± 1.62^{de}	77.86 ± 3.30^{d}
8	281.31 ± 15.05^{e}	2.38 ± 0.18^{a}	45.59 ± 2.76^{a}	88.56 ± 1.10^{c}
9	304.59 ± 11.24^{d}	2.13 ± 0.06^{b}	40.11 ± 6.67^{bcd}	89.70 ± 8.73^{c}
10	319.81 ± 22.82^{c}	2.15 ± 0.06^{b}	44.31 ± 6.93^{ab}	99.14 ± 15.42^{b}
11	368.00 ± 13.72^{b}	2.13 ± 0.16^{b}	37.47 ± 8.03^{cde}	110.41 ± 23.47^{a}
12	394.30 ± 15.20^{a}	2.10 ± 0.05^{b}	41.34 ± 1.44^{abc}	110.96 ± 4.86^{a}

Note: Mean values with different letters within each line are significantly different ($p < 0.05$) with respect to processing.

3.1.6. Microscopic structural analysis

Fig. 2 depicts the scanning electron microscopic images of the shrimp muscles during drying. Upon blanching, the shrimp muscle appeared intact, exhibiting a clear texture, tight arrangement, and small spaces between fibers. However, drying disrupts the integrity of the muscle fibers. Changes in microstructure during drying are associated with water migration. After 4 h of drying, the muscle fibers were significantly contracted and presented wide interfiber gaps, water continues to migrate to the muscle fibers and meat surface, and the signal peak area of immobilized water plummets. After drying for 8 h, the weakly bound water trapped in the highly organized tissues continued to evaporate, with decreasing A_{21} values. The muscle fiber contraction increased, and the fascicles became thinner and fractured. The fiber network structure was destroyed after 12 h of drying, loosening the overall spatial structure. Qi et al. (2021) observed that heat-induced protein denaturation during drying induces protein crosslinking and aggregation, resulting in muscle fiber compaction, fibrin dehydration, larger interfiber spaces, and altered shrimp product quality. Along with the protein structure-related changes, the interior moisture mobilization rate increased. Finally, the rapid evaporation enlarged the interfiber spaces and loosened the overall structure.

3.2. Analysis of the protein changes during shrimp drying

3.2.1. TCA-soluble peptides

TCA-soluble peptides are often used as protein degradation indicators. In particular, shrimp contains small peptides, free amino acids, and other nonprotein nitrogenous substances, such as free bases (pyrimidines and pyridines) and nucleic acids (Zhu et al., 2022). Higher TCA-soluble peptide levels indicate higher-level protein degradation. Fig. 3 presents the TCA-soluble peptide-related changes during shrimp drying. The TCA-soluble peptide content gradually increased from 0.65 mg/g (fresh) to 0.85 mg/g (after blanching), reaching a maximum value of 2.52 mg/g after drying for 12 h. These results indicate that drying gradually degraded the component proteins, potentially attributed to

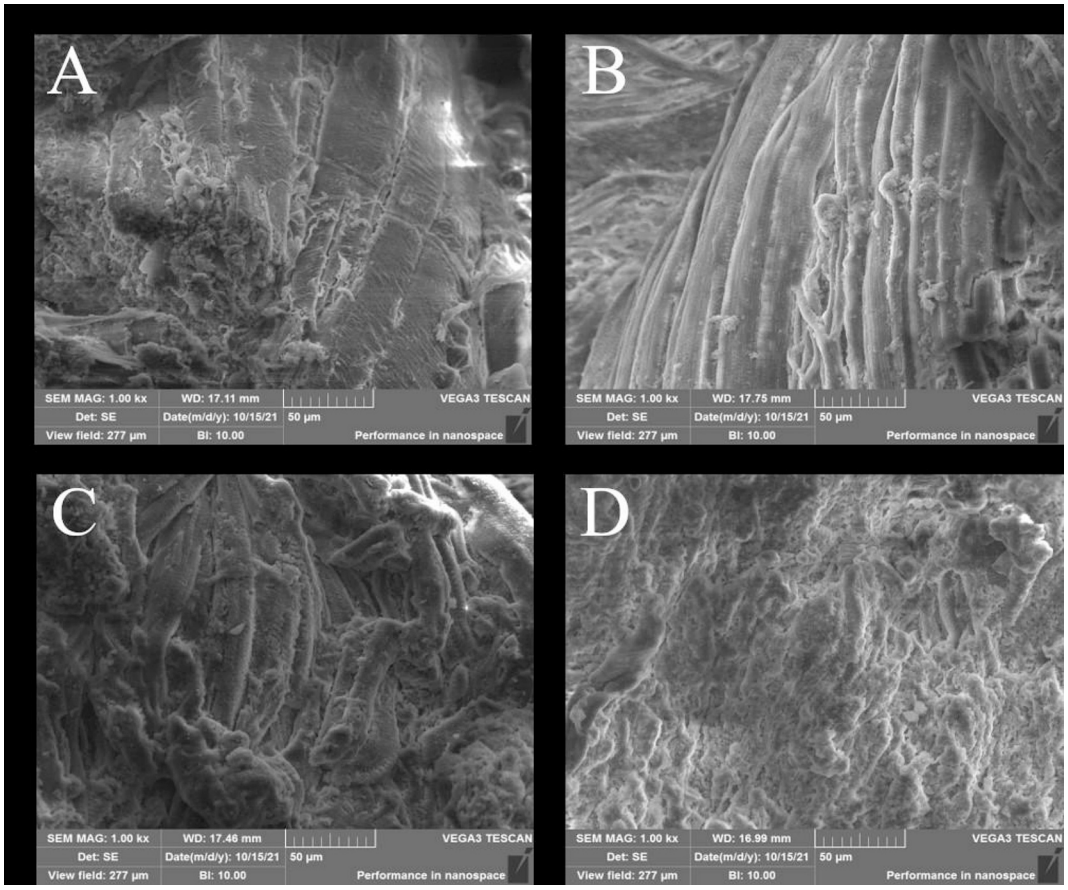

Fig. 2. Changes in the microstructure of *Penaeus vannamei* during the drying process (magnification: 1000×) [A: Boiled shrimp; B–D: Shrimp samples after drying for 4 h (B), 8 h (C), 12 h (D)].

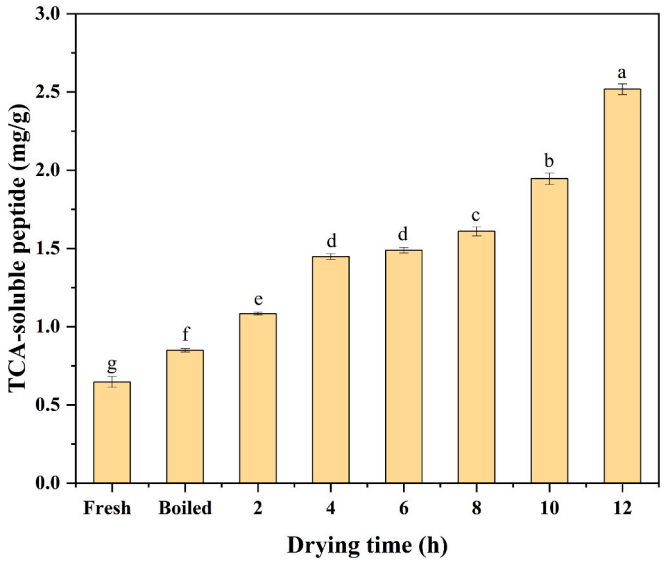

Fig. 3. Changes in the TCA-soluble peptide content in *Penaeus vannamei* during the drying process.

the cooking process, which induces protein denaturation. This denaturation leads to a partially unfolded protein structure, exposing more hydrolysis sites and promoting protein degradation into peptides. With gradually extended subsequent drying times and rapid water loss, this ultimately results in a gradual increase in soluble peptide content. Nie, Lin, and Zhang (2014) obtained similar results, establishing that endogenous enzymes contribute to soluble peptide release from TCA, thereby increasing their content. High-temperature blanching might deactivate endogenous shrimp enzymes during the initial drying phase. However, with a short blanching, the enzymes presumably remain partially active, increasing the TCA-soluble peptide content (Saengsuk et al., 2021). During the final drying phase, protein denaturation reduces water retention, free and immobilized water evaporates completely, and a large amount of water is lost, enabling rapid moisture dissipation and increasing TCA-soluble peptide abundance.

3.2.2. *SDS-PAGE analysis*

Drying altered shrimp myofibrillar protein molecular weight (Fig. 4). The characteristic myofibrillar protein bands include myosin heavy chain (MHC, 220 kDa), α-actin (94 kDa), tropomyosin (80 kDa), troponin (75 kDa), actin (43 kDa), troponin T (37 kDa), troponin I (23 kDa), and myosin light chain (< 20 kDa) (Fuente-Betancourt, Garca-Carreo, Toro, Crdova-Murueta, & Lugo-Snchez, 2009). Fresh shrimps display a complete myofibrillar protein composition with primary bands in the 35–250-kDa range, demonstrating a relatively complete protein composition in the untreated shrimp samples. After boiling the samples, only the 20-, 35-, and 40-kDa bands were observed, whereas those corresponding to myosin heavy chain, α-actin, and tropomyosin disappeared. This result indicates that the heating treatment degraded the macromolecular myofibrillar proteins, such as MHC, α-actinin and promyosin, and that troponin was degraded to produce troponin T and troponin I. The degradation of troponin was also observed in the myofibrillar proteins. During subsequent drying, the degradation of troponin and actin bands continued, resulting in low-molecular weight bands. In contrast, troponin T, troponin I, and myosin light chain bands became darker, indicating further degradation of myofibrillar proteins

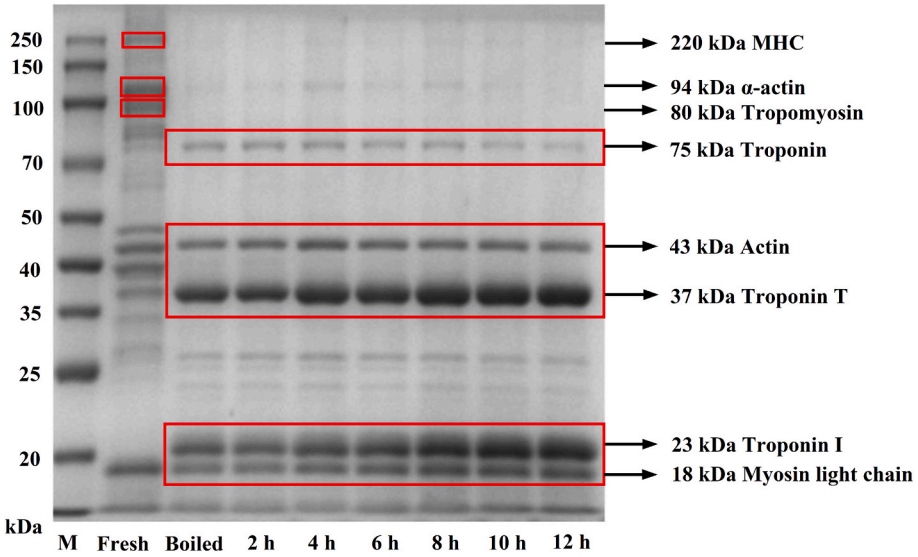

Fig. 4. Changes in the SDS-PAGE protein profile of *Penaeus vannamei* during the drying process.

into small molecular weight protein fragments. This process resulted in an increase in the near-10-kDa protein band concentrations in Fig. 4. The SDS-PAGE results indicate that most shrimp proteins were heat intolerant and degraded during drying, indicated by the TCA-soluble peptide content-related changes.

3.2.3. Protein carbonyl-group analysis

Fig. 5A illustrates protein carbonyl group-related alterations during shrimp drying. Protein carbonyl groups are among the most important protein oxidation indicators in food products. Carbonyl groups are formed by free radical-sensitive amino acid side chain and peptide chain destruction (Guyon, Meynier, & de lamballerie, M., 2016). The spatial structure of shrimp protein denaturation was altered upon boiling, leading to peptide chain stretching and rendering the peptide bonds unstable. During the subsequent drying process, the peptide chains broke to form carbonyl groups, thereby significantly increasing protein carbonyl group abundance from 1.13 to 2.22 nmol/mg ($p < 0.05$). Similarly, Chen et al. (2022) also described an increased protein carbonyl compound content in *Chlamys nobilis* adducts upon drying. They suggested that lipid oxidation products, such as lipid-derived radicals and hydroperoxides, could promote protein carbonylation and interact with proteins to form complexes. These results suggest that lipid oxidation might influence protein oxidation during drying.

3.2.4. Total sulfhydryl group analysis

Next, we studied total sulfhydryl group-related changes during shrimp drying (Fig. 5B), representing further important protein oxidation indicators in food products (Xu et al., 2023). Sulfhydryl groups significantly affect protein functional properties. The total sulfhydryl group levels decreased significantly from 2.79 μmol/g (fresh) to 1.10 μmol/g (after blanching). With increasing drying times, the total sulfhydryl group content further decreased to 0.36 μmol/g, potentially due to the thermal denaturation of the sulfhydryl groups in the cysteine residues after boiling, structural stretching exposing these groups to the surface, and the maintained oxidation of the exposed groups during subsequent drying, thereby reducing the sulfhydryl content throughout the process. Ko, Yu, and Hsu (2007) investigated compositional changes in tilapia after heat treatment and reported that protein sulfhydryl groups were gradually became exposed to reactive oxygen species during heating, which subsequently reacted with the sulfhydryl groups, resulting in sulfhydryl group conversion into disulfide bonds. In addition, the interior denaturation of partial protein molecules, sulfhydryl group oxidation within the molecules, and disulfide formation could reduce the total sulfhydryl content (Shi et al., 2017), potentially explaining the observed reduction.

3.2.5. Intermolecular forces

Fig. 5C–F highlights the changes in the protein intermolecular forces during drying. Intermolecular force proportions in fresh shrimp proteins are as follows: ionic > hydrogen > disulfide > and hydrophobic bonds. Ionic and hydrogen bond proportions rapidly decreased to 15.89% and 12.89% (after blanching), reaching 10.72% and 9.05% after drying, respectively. In contrast, disulfide and hydrophobic bond proportions increased to 19.38% and 28.19% (after drying), respectively, with disulfide bonds significantly increasing to 27.23% after blanching. Xu et al. (2023) also described reduced ionic and hydrogen contents and increased hydrophobic and disulfide bond contents when investigating chemical force-related changes in shrimp during hot air drying. These results reveal hydrophobic and disulfide bond dominance in the intermolecular forces that maintained shrimp protein structure stability during drying.

Ionic bonds are distributed on the surface of proteins, formed by attractive forces between ions, requiring a certain amount of moisture to facilitate ionic interactions. Weakly bonded ionic bonds of prawns are easily broken during boiling, leading to a rapid decrease in their content. During drying, the proportion of ionic bonds continues to decrease owing to water evaporation, heating, and other factors, which also reduce ionic interactions. Hydrogen bonds represent noncovalent interactions and are among the most important forces that maintain spatial protein structural stability. Heat treatment alters the thermal state of motion of the molecules and affects the formation of hydrogen bonds, which become more difficult to form owing to the evaporation of water as the drying time increases. This leads to the breaking of hydrogen bonds between amino and acyl groups in the protein polypeptide chain. Hydrophobic bonds or interactions are established when hydrophobic amino acid side chains or groups in protein molecules interact with each other (Mao et al., 2016). During the heating process, protein enhanced the hydrophobic interactions among the neighboring nonpolar fragments of the polypeptide, leading to increased exposure of hydrophobic residues. Subsequently hydrophobicity significantly increased after the synergistic drying treatment. Disulfide bonds are covalent bonds formed upon the oxidation of two thiol groups, which are important for secondary and tertiary protein structures (Mao et al., 2022). Structural changes in protein denaturation after cooking of shrimp resulted in the oxidation of most of the buried sulfhydryl groups and the formation of disulfide bonds, and the sulfhydryl groups

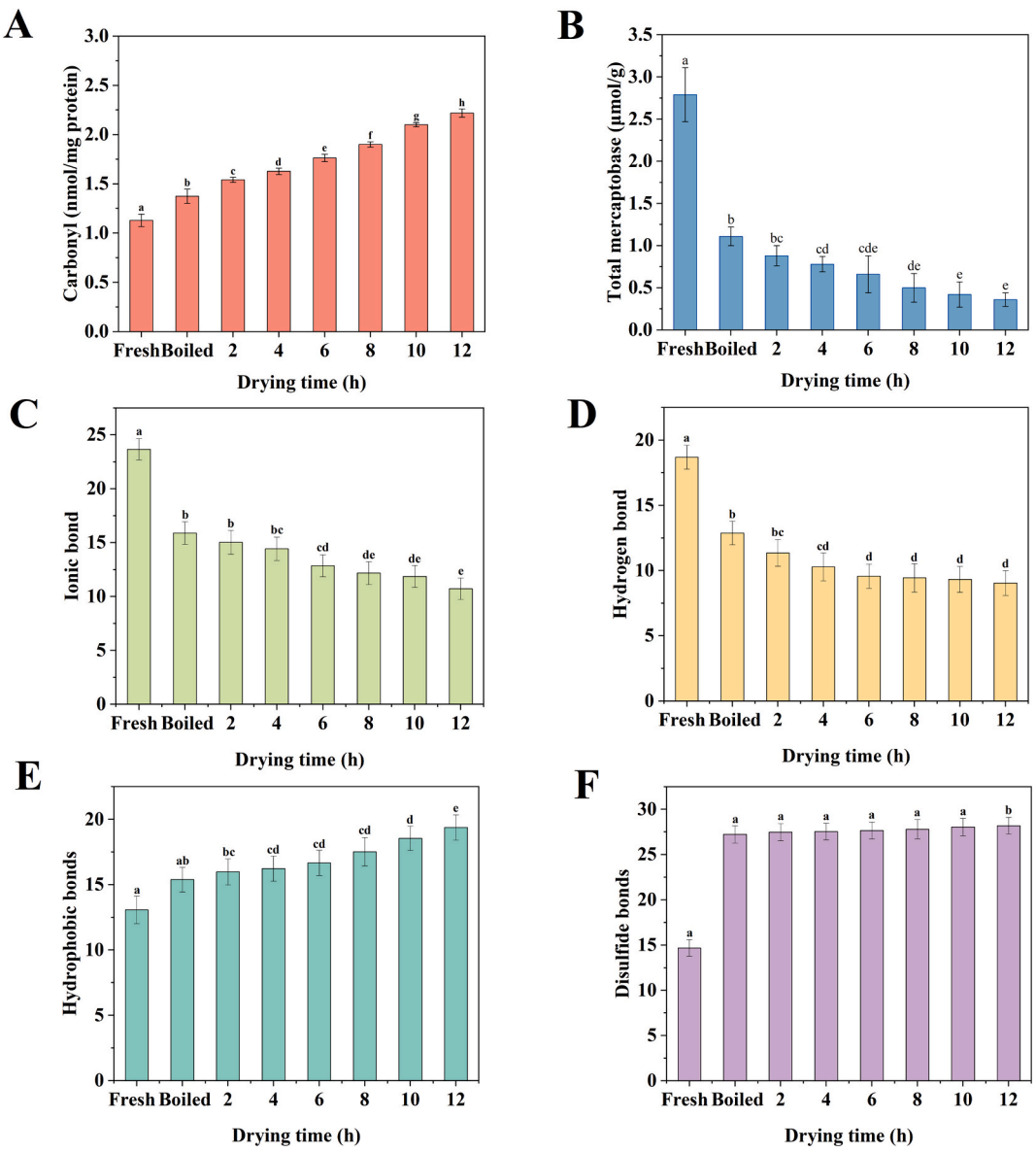

Fig. 5. Changes in the content of protein carbonyls, total sulfhydryl groups, and chemical forces in *Penaeus vannamei* during the drying process. A: protein carbonyl content; B: total sulfhydryl content; C: ionic bond; D: hydrogen bond; E: hydrophobic bonds; F: disulfide bonds.

continued to be oxidized after drying, consistent with the associated changes in total sulfhydryl content.

3.3. Sample quality and protein characteristics-related correlation analysis

Pearson's correlation analysis was performed to determine the correlation between shrimp quality- and protein content-related changes during solar drying (Fig. 6A). The texture indicator (hardness, elasticity, stickiness, and chewiness) and protein-related changes exhibited a significant correlation during shrimp drying. Meanwhile, the changes in the color parameters (L^*, a^*, and b^*) exhibited a lower correlation with protein-related indicators, although they were significantly positively correlated with disulfide-bond changes ($p < 0.01$; Pearson's coefficients: 0.917, 0.918, and 0.894, respectively) and significantly negatively correlated with changes in the sulfhydryl groups (Pearson's coefficients: −0.788, −0.792, and − 0.760, respectively). The L^* and a^* values were significantly negatively correlated with the changes in the ionic and hydrogen bonds ($p < 0.05$; Pearson's coefficients: −0.708, −0.743, −0.724, and − 0.729, respectively). Sulfhydryl groups are readily oxidized into disulfide bonds during drying. The relatively weak binding of the ionic bonds is broken, and the continuous water evaporation from the shrimps leads to hydrogen bond breakage. Moreover, drying could induce myoglobin to undergo oxidation-related color changes. Proteins could degrade into peptides and amino acids, which could participate in the Maillard reaction, resulting in product color darkening. Oxidation might also alter protein and lipid structures, resulting in volume reduction, moisture loss, and additional color changes (Rodrigues et al., 2017).

As Fig. 6A illustrates that the texture indicators (i.e., hardness, elasticity, stickiness, and chewiness) significantly positively ($p < 0.05$) were correlated with the changes in the TCA-soluble peptides, carbonyl groups, and hydrophobic bonds, although they were significantly negatively ($p < 0.05$) correlated with the total sulfhydryl groups, ionic bonds, and hydrogen bonds. Elasticity significantly positively correlated with the disulfide bond changes ($p < 0.01$; Pearson coefficient: 0.897). Amino acids might form more hydrophobic bonds during protein denaturation, thereby increasing product hardness and chewiness. Moreover, carbonyl groups might enhance hydrogen bonding and hydrophobic interactions between the protein chains, resulting in a sticky

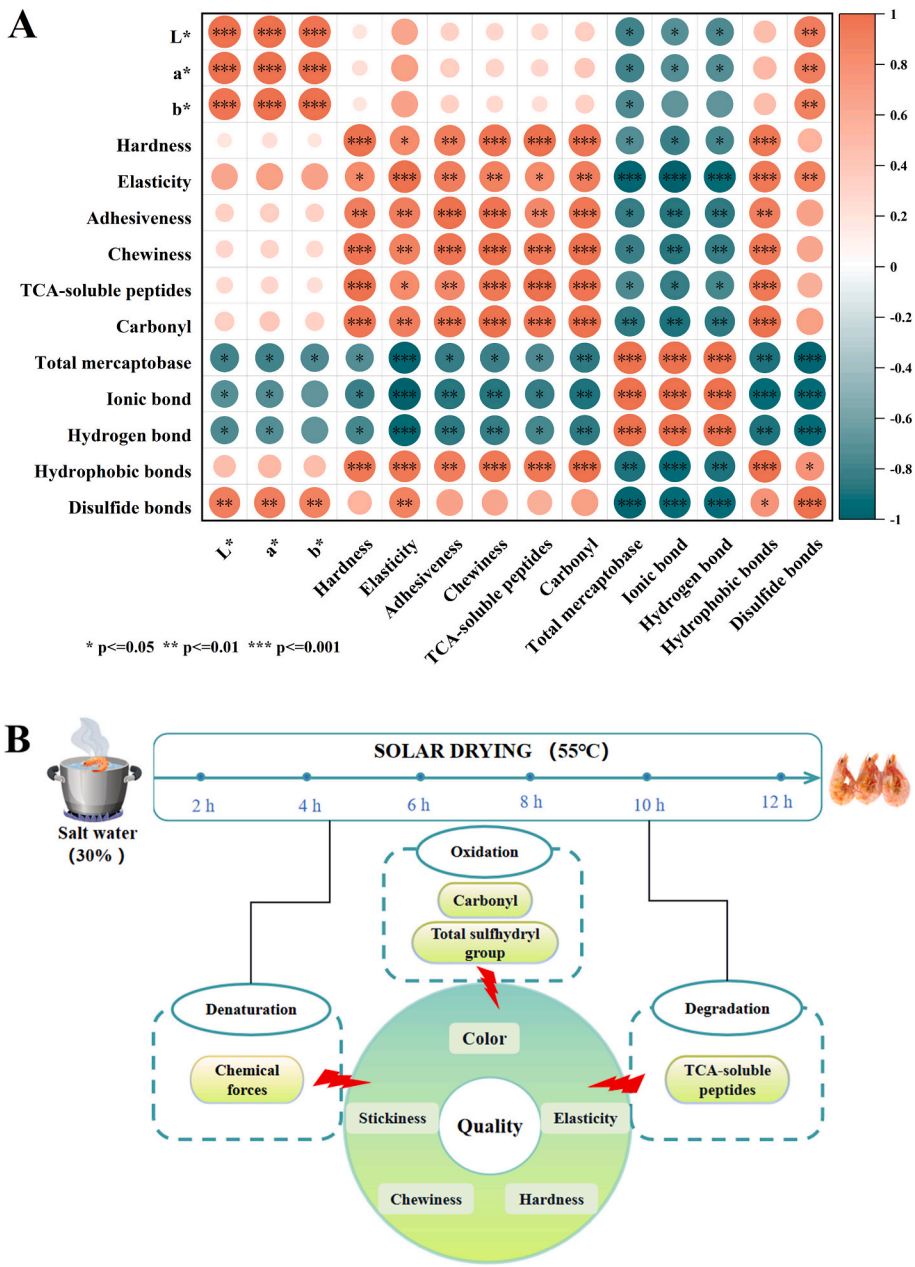

Fig. 6. Correlation analysis of the protein changes and quality of *Penaeus vannamei* samples during the drying process (A), and correlation diagram (B).

and elastic product (Gao et al., 2016). The hydrogen-bond disruption could impair the connections between the protein chains, reducing dried shrimp product hardness and elasticity. Moreover, it can interfere with the interaction between protein molecules, resulting in a less sticky and chewy product. Total sulfhydryl group reduction might disrupt the protein structures. The disulfide bonds connect cysteine residues in the protein chains, potentially enhancing protein stability and product elasticity (Duan et al., 2023). Similar results were reported by Xu et al. (2023) who investigated the quality and protein correlations during hot air drying. Our results demonstrated that protein oxidation mainly affected the color change during the shrimp drying process, while shrimp meat texture was more closely related to protein degradation and denaturation.

4. Conclusion

In this study, we performed an in-depth analysis of shrimp quality and protein changes under solar drying. Subsequently, we analyzed the correlations between color, texture, and protein changes. We observed that several protein- and quality-related parameters changed during sample drying. As the moisture content decreased during drying, the protein and fat contents increased. The shrimp color properties (i.e., L^*, a^*, and b^* values) gradually decreased, and the hardness and chewiness increased significantly. The TCA-soluble peptide contents increased. Our SDS-PAGE results revealed that several protein bands vanished, whereas the troponin and troponin T band intensities increased, and the troponin I band appeared, demonstrating triggered protein degradation upon drying. The carbonyl-group concentration, representing protein oxidation, increased, whereas the overall sulfhydryl-group level decreased, demonstrating that drying induced protein denaturation. The drying process induced conformational changes in the shrimp proteins with significantly decreasing proportions of ionic and hydrogen bonds and increasing hydrophobic and disulfide bonds, demonstrating a loosened molecular structure during drying. Our correlation analysis revealed

that protein degradation, oxidation, and structural changes affected the sample color and texture. Therefore, our study provides a theoretical basis for evaluating how solar drying affects shrimp product quality.

CRediT authorship contribution statement

Xinyue Pan: Writing – original draft, Conceptualization. **Jiarong Wang:** Software, Methodology. **Wenya Xu:** Data curation. **Jie Wang:** Visualization, Validation, Investigation. **Jianfeng Sun:** Validation, Software. **Wenxiu Wang:** Writing – review & editing, Supervision. **Yiwei Tang:** Writing – review & editing, Supervision.

Declaration of competing interest

The authors declare that they have no known competing financial interests or personal relationships that could have appeared to influence the work reported in this paper.

Data availability

The authors do not have permission to share data.

Acknowledgements

This research was supported by the Natural Science Foundation (Grant No. 32001732), Seafood Deep Processing and Market Development Innovation Team in Characteristic Seafood Industry of Modern Agriculture Industry Technology System of Hebei Province (grant no. HBCT2024290206), and the National Key Research and Development Program of China (Grant No. 2018YFD0901004).

Appendix A. Supplementary data

Supplementary data to this article can be found online at https://doi.org/10.1016/j.fochx.2024.101696.

References

Akonor, P. T., Ofori, H., Dziedzoave, N. T., & Kortei, N. K. (2016). Drying characteristics and physical and nutritional properties of shrimp meat as affected by different traditional drying techniques. *International Journal of Food Science, 2016*, Article 7879097.

Beuchat, L. R., Komitopoulou, E., Beckers, H., Betts, R. P., Bourdichon, F., Fanning, S., … Kuile, B. H. T. (2013). Low-water activity foods: Increased concern as vehicles of foodborne pathogens. *Journal of Food Protection, 76*(1), 150–172.

Chen, Z. Q., Zhu, Y. H., Cao, W. H., Zhou, L. J., Zhang, C. H., Qin, X. M., … Gao, J. L. (2022). Novel insight into the role of processing stages in nutritional components changes and characteristic flavors formation of noble scallop chlamys nobilis adductors. *Food Chemistry, 378*, Article 132049.

Dong, Z. J., Sun, L. P., Qi, X. P., Zhang, H. X., Qu, G. X., & Wu, M. L. (2020). Quality changes of *Penaeus vannamei* during cold air drying process. *Food Research and Development, 41*(8), 45–49.

Duan, W. W., Qiu, H., Htwe, K. K., Wei, S., Liu, Y., Wang, Z. F., … Liu, S. C. (2023). Changes in advanced protein structure during dense phase carbon dioxide induced gel formation in golden pompano surimi correlate with gel strength. *Frontiers in Sustainable Food Systems, 7*.

Duppeti, H., Manjabhatta, S. N., & Kempaiah, B. B. (2023). Physicochemical, structural, functional and flavor adsorption properties of white shrimp (*Penaeus vannamei*) proteins as affected by processing methods. *Food research international (Ottawa, Ont.), 163*, Article 112296.

Emilia Latorre, M., & Ezequiel Velazquez, D. (2021). Effects of thermal treatment on collagen present in bovine M. Semitendinosus intramuscular connective tissue. Analysis of the chemical, thermal and mechanical properties. *Food Structure-Netherlands, 27*.

Fuente-Betancourt, G. D. L., Garca-Carreo, F., Toro, M. A. N. D., Crdova-Murueta, J. H., & Lugo-Snchez, M. E. (2009). Protein solubility and production of gels from jumbo squid. *Journal of Food Biochemistry, 33*(2), 273–290.

Gao, R. C., Feng, X. P., Li, W. W., Yuan, L., Ge, J., Lu, D. L., … Yu, G. (2016). Changes in properties of white shrimp (*Litopenaeus vannamei*) protein during thermal denaturation. *Food Science and Biotechnology, 25*(1), 21–26.

Guo, Q., Xu, S., Liu, H. M., Wang, C. X., Qin, Z., & Wang, X. D. (2022). Effects of roasting temperature and duration on color and flavor of a sesame oligosaccharide-protein complex in a Maillard reaction model. *Food Chemistry: X, 16*.

Guo, X. X., Wang, W. H., Liu, Y., Ran, G. W., Zhang, H. Y., Guo, H. F., & Wang, H. (2017). Study on the technology optimization of the solar drying energy consumption in *Penaeus vannamei* by response surface methodology. *Food Research and Development, 38*(21), 91–96.

Guyon, C., Meynier, A., & de lamballerie, M.. (2016). Protein and lipid oxidation in meat: A review with emphasis on high-pressure treatments. *Trends in Food Science & Technology, 50*, 131–143.

Haritha, D., Nakkarike Manjabhatta, S., & Bheemanakere Kempaiah, B. (2023). Physicochemical, structural, functional and flavor adsorption properties of white shrimp (*Penaeus vannamei*) proteins as affected by processing methods. *Food Research International, 163*, 112296.

Ko, W. C., Yu, C. C., & Hsu, K. C. (2007). Changes in conformation and sulfhydryl groups of tilapia actomyosin by thermal treatment. *Lebensmittel-Wissenschaft und Technologie, 40*(8), 1316–1320.

Koutina, G., Jongberg, S., & Skibsted, L. H. (2012). Protein and lipid oxidation in parma ham during production. *Journal of Agricultural and Food Chemistry, 38*, 9737–9745.

Li, D. Y., Liu, Z. Q., Liu, B., Qi, Y., Liu, Y. X., Liu, X. Y., … Fereidoon, S. (2020). Effect of protein oxidation and degradation on texture deterioration of ready-to-eat shrimps during storage. *Journal of Food Science, 85*(9), 2673–2680.

Li, D. Y., Zhou, D. Y., Yin, F. W., Dong, X. P., & Shahidi, F. (2020). Impact of different drying processes on the lipid deterioration and color characteristics of *Penaeus vannamei*. *Journal of the Science of Food and Agriculture, 100*(6).

Li, D. Y., Zhou, D. Y., Yin, F. W., Dong, X. P., Xie, H. K., Liu, Z. Y., … Shahidi, F. (2020). Impact of different drying processes on the lipid deterioration and color characteristics of *Penaeus vannamei*. *Journal of the Science of Food and Agriculture, 100*(6), 2544–2553.

Li, M., Guan, Z. Q., Ge, Y. T., Zhang, X. Y., & Ling, C. M. (2020). Effect of pretreatment on water migration and volatile components of heat pump dried tilapia fillets. *Drying Technology, 38*(14), 1828–1842.

Li, W. S., Zhu, Q. Q., Sun, J. C., Sang, W. G., & Yang, F. Y. (2016). Effect of different drying methods on the quality of white shrimps. *Journal of Food Science and Biotechnology, 35*(5), 543–548.

Li, Z. P., Zhou, X. J., Zhang, B., Su, L. J., & Shui, S. S. (2021). Changes in protein characteristics of minced shrimp (*Litopenaeus vannamei*) meat during deep-frozen storage. *Modern Food Science and Technology, 37*(1), 117–124.

Mao, M., Jia, R., Gao, Y., Yang, W., Tong, J., & Xia, G. (2022). Effects of innovative gelation and modified tapioca starches on the physicochemical properties of surimi gel during frozen storage. *International Journal of Food Science and Technology, 57*(10), 6591–6601.

Mao, W., Li, X., Fukuoka, M., Liu, S., Ji, H., & Sakai, N. (2016). Study of Ca^{2+}-ATPase activity and solubility in the whole kuruma prawn (*marsupenaeus japonicus*) meat during heating: Based on the kinetics analysis of myofibril protein thermal denaturation. *Food and Bioprocess Technology, 9*(9), 1511–1520.

Niamnuy, C., Devahastin, S., & Soponronnarit, S. (2007). Effects of process parameters on quality changes of shrimp during drying in a jet-spouted bed dryer. *Journal of Food Science, 72*(9), E553–E563.

Nie, X., Lin, S., & Zhang, Q. (2014). Proteolytic characterisation in grass carp sausage inoculated with *Lactobacillus plantarum* and *Pediococcus pentosaceus*. *Food Chemistry, 145*, 840–844.

Qi, X., Mao, J. L., Yao, H., Qi, H., Wu, T. X., Shui, S. S., & Zhang, B. (2021). Effect of protein oxidation on the quality attributes of *Solenocera crassicornis* muscle. *Food Science, China, 42*(18), 15–21.

Qin, J. Y., Wang, Z. H., Wang, X. C., & Shi, W. Z. (2020). Effects of microwave time on quality of grass carp fillets processed through microwave combined with hot-air drying. *Food Science & Nutrition, 8*(8), 4159–4171.

Rodrigues, B. L., Costa, M. P. D., Frasão, B. D. S., Silva, F. A. D., Mársico, E. T., Alvares, T. D. S., & Conte-Junior, C. A. (2017). Instrumental texture parameters as freshness indicators in five farmed brazilian freshwater fish species. *Food Analytical Methods, 10*(11).

Saengsuk, N., Laohakunjit, N., Sanporkha, P., Kaisangsri, N., Selamassakul, O., Ratanakhanokchai, K., & Uthairatanakij, A. (2021). Physicochemical characteristics and textural parameters of restructured pork steaks hydrolysed with bromelain. *Food Chemistry, 361*.

Shaheed, R., Jafor, B. A., Nazrul, I., & Kamal, M. D. (2009). Optimization of marine fish drying using solar tunnel dryer. *Journal of Food Processing and Preservation, 33*(1), 47–59.

Shi, J., Zhang, L. T., Lu, H., Shen, H. X., Yu, X. P., & Luo, Y. K. (2017). Protein and lipid changes of mud shrimp (*Solenocera melantho*) during frozen storage: Chemical properties and their prediction. *International Journal of Food Properties, 20*, 2043–2056.

Tong, J., Jia, R., Xia, G., Zhang, X., Zhang, S., Wei, H., & Yang, W. (2023). Influence mechanisms of different setting time at low temperature on the gel quality and protein structure of Solenocera crassicornis surimi. *Food Bioscience*, 51.

Wang, J., Che, B., & Sun, C. (2022). Spatiotemporal variations in shrimp aquaculture in China and their influencing factors. *Sustainability, 14*(21).

Wang, S. W., Jin, J. Y., Suo, R., Wang, Y. J., Wang, J., Wang, W. X., … Bimal, C. (2022). Evaluation of solar drying on drying behaviour and drying kinetics of *Penaeus vannamei*. *Journal of Aquatic Food Product Technology, 31*(4), 344–360.

Wang, Y. Q., Zhang, M., & Mujumdar, A. S. (2011). Trends in processing technologies for dried aquatic products. *Drying Technology, 29*(4), 382–394.

Xu, W. Y., Ma, Q. Y., Wang, J. R., Sun, J. F., Tang, Y. W., Wang, J., & Wang, W. X. (2023). Study on the relationship between protein and quality changes during hot air drying of shrimp (*Penaeus vannamei*). *Food Science, 44*(15), 40–48.

Xu, W. Y., Zhang, F., Wang, J. R., Ma, Q. Y., Sun, J. F., Tang, Y. W., … Wang, W. X. (2022). Real-time monitoring of the quality changes in shrimp (*Penaeus vannamei*) with hyperspectral imaging technology during hot air drying. *Foods, 11*(20), 3179.

Zhang, C., Shi, R., Liu, W., Xu, Z., Mi, S., Sang, Y., … &Wang, X. (2023). Effect of different thermal processing methods on sensory, nutritional, physicochemical and structural properties of *Penaeus vannamei*. *Food Chemistry, 438*, 138003-138003.

Zhu, C., Jiao, D. X., Sun, Y., Chen, L. H., Meng, S. Y., Yu, X. N., … Liu, H. M. (2022). Effects of ultra-high pressure on endogenous enzyme activities, protein properties, and quality characteristics of shrimp (*Litopenaeus vannamei*) during iced storage. *Molecules, 27*(19), 6302.

Zhu, N., Zhang, S. L., Zhao, B., Wu, Q. R., & Qiao, X. L. (2020). Effect of processing on protein degradation and quality of emulsion sausages. *Food Bioscience, 37*(3), Article 100685.